

BraWL: Simulating the thermodynamics and phase stability of multicomponent alloys using conventional and enhanced sampling techniques

Hubert J. Naguszewski¹, Livia B. Pártay², David Quigley¹, and Christopher D. Woodgate³✉

¹ Department of Physics, University of Warwick, UK^{ROR} ² Department of Chemistry, University of Warwick, UK^{ROR} ³ School of Physics, University of Bristol, UK^{ROR} ✉ Corresponding author

DOI: [10.xxxxxx/draft](https://doi.org/10.xxxxxx/draft)

Software

- [Review](#) ✉
- [Repository](#) ✉
- [Archive](#) ✉

Editor: Jeff Gostick ✉ 

Reviewers:

- [@amkrajewski](#)
- [@sudarshanv01](#)

Submitted: 13 May 2025

Published: unpublished

License

Authors of papers retain copyright and release the work under a Creative Commons Attribution 4.0 International License ([CC BY 4.0](https://creativecommons.org/licenses/by/4.0/)).

Summary

Many technologically relevant materials, both structural and functional, are ‘alloys’ – systems in which two or more (typically) metallic elements are combined to produce a new material with desirable physical properties. In a substitutional alloy, there is a fixed underlying crystal lattice, while the probability of a given constituent element of the alloy occupying a particular lattice site is determined by thermodynamic considerations. In accordance with these considerations, atoms in an alloy can arrange themselves differently depending on the precise chemical composition and processing conditions. Frequently, a mixture of elements will form a regular crystalline lattice with substitutional disorder (a ‘solid solution’) at high temperature, before atomic short- and long-range order emerges as the material is cooled. The nature of atomic arrangements in a material determines many important physical properties. For a given combination of elements, it is therefore crucial to understand the nature of atomic ordering in a material, as well as the temperature at which it emerges upon cooling, to guide materials processing strategies. One physically intuitive model for the internal energy of an alloy is the Bragg-Williams model, which assumes that atoms in the alloy interact in a pairwise manner. Crucially, the effective pair interactions (EPIs) which appear in the Bragg-Williams Hamiltonian can be obtained *ab initio* using density functional theory (DFT) calculations. When appropriate sampling techniques are applied to the Bragg-Williams model, it is possible to explore the configuration space of a given alloy in detail and determine equilibrium phases as a function of temperature, leading to construction of phase diagrams. Here, we present BraWL, a Fortran package implementing a range of conventional and enhanced sampling algorithms for exploration of the phase space of the Bragg-Williams model, facilitating study of diffusional solid-solid transformations in binary and multicomponent alloys. These sampling algorithms include Metropolis-Hastings Monte Carlo, Wang-Landau sampling, and Nested Sampling. We demonstrate the capabilities of the package by applying it to some prototypical binary and multicomponent alloys, including high-entropy alloys.

Statement of need

The Fortran package BraWL facilitates simulation of the thermodynamics and phase stability of both binary and multicomponent alloys. It achieves this by providing implementation of both the Bragg-Williams Hamiltonian (a lattice based model expressing the internal energy of an alloy as a sum of atom-atom effective pair interactions) concurrently with a range of conventional and enhanced sampling techniques for exploration of the alloy configuration space. The result is a package which can determine phase equilibria as a function of both temperature and alloy composition, which leads to the construction of alloy phase diagrams.

42 Additionally, the package can be used for extraction of representative equilibrated atomic
43 configurations for visualisation, as well as for use in complementary modelling approaches. An
44 in-depth discussion of the background, underlying theory, and technical details of the sampling
45 algorithms implemented in the package is given by Naguszewski et al. (2025).

46 There are a range of existing packages capable of simulating alloy phase equilibria, both open-
47 and closed-source. Examples of widely-used such packages include ATAT (Van De Walle et al.,
48 2002), ICET (Ångqvist et al., 2019) and CELL (Rigamonti et al., 2024), though all of these
49 focus primarily on implementation of a generalised cluster expansion, rather than the simpler
50 form of the Bragg-Williams Hamiltonian. To our knowledge, there is no open-source package
51 specifically focussing on the implementation of a range of sampling algorithms applied to the
52 Bragg-Williams model. We therefore believe that BraWi fills a gap in the capabilities of the
53 current alloy software ecosystem. Additionally, we hope that the modular way in which the
54 package is constructed could enable implementation of more complex Hamiltonians, as well as
55 further sampling algorithms in addition to those detailed below, in due course.

56 The Bragg-Williams Hamiltonian

57 A physically intuitive, lattice-based model for the internal energy of a substitutional alloy is
58 the Bragg-Williams model (Bragg & Williams, 1934, 1935), which assumes that the internal
59 energy of an alloy takes a simple, pairwise form. We specify a particular arrangement of atoms
60 by a discrete set of site occupation numbers, $\{\xi_{i\gamma}\}$, where $\xi_{i\gamma} = 1$ if lattice site i is occupied
61 by an atom of species γ and $\xi_{i\gamma} = 0$ otherwise. The Bragg-Williams Hamiltonian then has the
62 form

$$H(\{\xi_{i\gamma}\}) = \frac{1}{2} \sum_{i\gamma; j\gamma'} V_{i\gamma; j\gamma'} \xi_{i\gamma} \xi_{j\gamma'}, \quad (1)$$

63 where $V_{i\gamma; j\gamma'}$ denotes the effective pair interaction (EPI) between an atom of chemical species
64 γ on lattice site i and an atom of chemical species γ' on lattice site j . (The factor of $\frac{1}{2}$
65 eliminates double-counting in the summation.) For a system of finite size, it is assumed that
66 periodic boundary conditions are applied in all coordinate directions.

67 Generally, the assumption is made that the EPIs are spatially homogeneous and isotropic,
68 and Equation 1 is therefore rewritten as

$$H(\{\xi_{i\gamma}\}) = \frac{1}{2} \sum_{i\gamma} \xi_{i\gamma} \left(\sum_n \sum_{j \in n(i)} \sum_{\gamma'} V_{\gamma\gamma'}^{(n)} \xi_{j\gamma'} \right), \quad (2)$$

69 where the sum over i remains a sum over lattice sites, but the sum over n denotes a sum over
70 the coordination shells (nearest-neighbours, next-nearest-neighbours, etc.) of the lattice. The
71 notation $n(i)$ is then used to denote the set of lattice sites which are n th nearest-neighbours
72 to site i . Then $V_{\gamma\gamma'}^{(n)}$ denotes the effective pair interaction between chemical species γ and γ'
73 on coordination shell n . It is reasonable to assume that, for most alloys, the strength of EPIs
74 will tail off quickly with decreasing distance, and the sum over n can be taken over the first
75 few coordination shells of the underlying lattice type being considered. (This is, of course,
76 equivalent to imposing some radial ‘cutoff’ on an interatomic potential.)

77 EPIs for the Bragg-Williams Hamiltonian can be obtained using a variety of methods, generally
78 those based on density functional theory. As examples of such methods, we highlight the
79 recovery of such interactions obtained by fitting to a set of DFT total energy evaluations on
80 alloy supercells (Liu et al., 2021; Zhang et al., 2020), the generalised perturbation method
81 (GPM) (Ducastelle & Gautier, 1976; Ruban et al., 2004), and techniques using the language
82 of concentration waves to describe the atomic-scale chemical fluctuations (Khan et al., 2016;
83 Singh et al., 2015). Once the EPIs for a given alloy composition are obtained, the phase stability
84 of a particular alloy can be examined using sampling techniques applied to the Bragg-Williams
85 model. This is the purpose of BraWi as presented in this work.

86 Sampling algorithms

87 BrawL implements a range of conventional and enhanced sampling algorithms for exploration
88 of the alloy configuration space. Throughout, the package defaults to performing *swaps* of
89 pairs of atoms in the simulation cell, to conserve the overall concentration of each chemical
90 species present in the simulation. At present, the implemented sampling algorithms are:

- 91 1. **The Metropolis-Hastings Monte Carlo algorithm.** The Metropolis-Hastings algorithm
92 allows for a system of interest to follow a chain of states which evolve to, and sample, an
93 equilibrium ensemble [Metropolis et al. (1953); landauguide2014]. It is a useful method
94 for obtaining the equilibrium state of a system at a given temperature.
- 95 2. **Wang-Landau sampling.** Wang-Landau sampling is a flat histogram method which
96 provides a means for high throughput calculation of phase diagrams for atomistic/lattice
97 model systems (Wang & Landau, 2001). The method allows for direct computation of
98 an estimate of the density of states in energy, $g(E)$, and hence the partition function
99 of a system of interest. From the partition function, thermodynamic quantities at any
100 temperature of interest can then be obtained provided one has prior knowledge of the
101 minimum and maximum energy relevant to those temperatures.
- 102 3. **Nested Sampling.** Nested sampling (NS) is powerful Bayesian inference technique
103 (Skilling, 2004, 2006) adapted to sample the potential energy surface of atomistic
104 systems (Ashton et al., 2022), giving direct access to the partition function at arbitrary
105 temperatures for comprehensive thermodynamic analysis, without relying on advance
106 knowledge of relevant structures or the range of energies accessible to them (Pártay et
107 al., 2010, 2021).

108 Physical quantities of interest

109 BrawL can extract a range of quantities of interest from a given alloy simulation. The relevant
110 quantities are:

- 111 ■ **Internal energy.** For a given lattice type, system size, alloy composition, and set of
112 atom-atom effective pair interactions, BrawL can evaluate the total energy associated
113 with the alloy configuration (Equation 1). At the time of writing, for speed, common
114 lattice types (fcc, bcc, simple cubic, etc.) are hard-coded, with the intention that the
115 range of implemented lattice types will be expanded over time as necessary.
- 116 ■ **Heat capacity.** The isochoric (fixed volume) heat capacity at a given temperature,
117 $C_V(T)$, is a useful quantity for identifying phase transitions, as a plot of the simulation
118 heat capacity as a function of temperature is expected to show a local peak at the
119 temperature at which the transition occurs. Within BrawL, the heat capacity is calculated
120 via

$$C_V(T) = \frac{\langle E^2 \rangle - \langle E \rangle^2}{k_B T^2},$$

121 where k_B is the usual Boltzmann constant, E is the simulation energy, and $\langle \cdot \rangle$ denote
122 thermodynamic averages obtained using the relevant sampling algorithm.

- 123 ■ **Atomic short-range order parameters.** To assess local atom-atom correlations in a
124 simulation, BrawL can calculate the Warren-Cowley atomic short-range order parameters
125 (Cowley, 1950, 1965), adapted to the multicomponent setting, defined as

$$\alpha_n^{\gamma\gamma'} = 1 - \frac{P_n^{\gamma\gamma'}}{c_{\gamma'}},$$

126 where n refers to the n th coordination shell, $P_n^{\gamma\gamma'}$ is the conditional probability of
127 an atom of type q neighbouring an atom of type p on shell n , and c_q is the total
128 concentration of atom type q . When $\alpha_n^{\gamma\gamma'} > 0$, p - q pairs are disfavoured on shell n

and, when $\alpha_n^{\gamma\gamma'} < 0$ they are favoured. The value $\alpha_n^{\gamma\gamma'} = 0$ corresponds to the ideal, maximally disordered solid solution.

- **Atomic long-range order parameters.** Over a simulation run (for example using the Metropolis algorithm), BraWL can calculate the average occupancy of a lattice site, *i.e.* the probability of an atom of a particular chemical species sitting on that site. This capability was first demonstrated on simulations of Fe-Ga alloys (Marchant et al., 2021).

Example Applications

BraWL has been used, with success, to study the phase behaviour of a range of binary and multicomponent alloys, for example the binary Fe-Ga system (Galfenol) (Marchant et al., 2021), the Fe-Ni system (Woodgate, Lewis, et al., 2024), the Cantor-Wu medium- and high-entropy alloys (Woodgate et al., 2023; Woodgate & Staunton, 2022), the refractory high-entropy alloys (Woodgate & Staunton, 2023, 2024), the $\text{Al}_x\text{CrFeCoNi}$ system (Woodgate, Marchant, et al., 2024), and the AlTiVNb and AlTiCrMo refractory high-entropy superalloys (Woodgate et al., 2025). The package has also been used to generate atomic configurations for training datasets for machine-learned interatomic potentials, for example for the prototypical austenitic stainless steel, $\text{Fe}_7\text{Cr}_2\text{Ni}$ (Shenoy et al., 2024).

As an example of the Metropolis-Hastings Monte Carlo algorithm, we consider its application to the binary FeNi alloy, first discussed by Woodgate, Lewis, et al. (2024). Figure 1 shows the internal energy and conditional pair probabilities (quantifying ASRO) of a simulation cell containing 256 atoms as a function of the number of Metropolis-Hastings ‘sweeps’, where a sweep refers to performing a number of trial Metropolis-Hastings moves equal to the number of atoms in the simulation cell. The simulation is performed at 300 K, below the alloy’s $L1_0$ disorder-order transition temperature. The $L1_0$ phase is a structure where 2/3 of the nearest neighbours of Fe (Ni) atoms are Ni (Fe) atoms, and where none of the next-nearest neighbours of Fe (Ni) atoms are Ni (Fe) atoms. It can be seen that this ordering is swiftly established as the number of Monte Carlo sweeps increases, albeit with some remaining thermal noise.

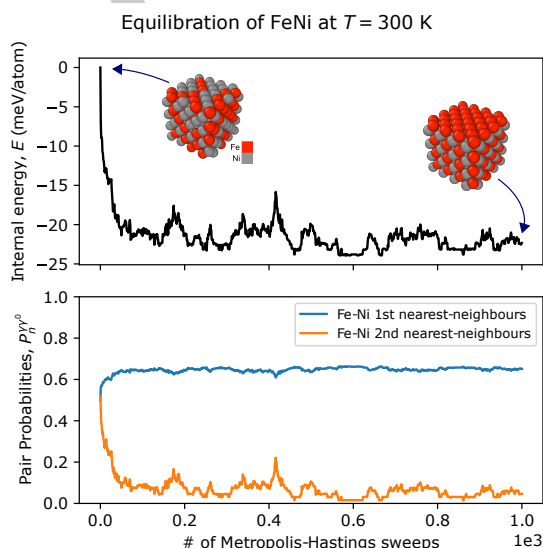


Figure 1: Evolution of the simulation internal energy (top panel) and conditional pair probabilities (bottom panel) for an $\text{Fe}_{0.5}\text{Ni}_{0.5}$ alloy as a function of the number of Metropolis-Hastings sweeps at a simulation temperature of $T = 300$ K. One ‘sweep’ is one trial move per atom in the system. Beyond approximately 100 sweeps, the system can be seen to have reached equilibrium, with $L1_0$ order established.

As an example of Wang-Landau sampling, we consider its application to the AlTiCrMo refractory

high-entropy superalloy, first discussed by Woodgate et al. (2025), for which results are shown in Figure 2. The top panel shows calculated energy probability distributions (histograms) at various temperatures, while the bottom panel shows the simulation heat capacity and evolution of the Warren-Cowley ASRO parameters as a function of temperature. The high-temperature peak in the heat capacity data is associated with the experimentally observed B2 crystallographic ordering.

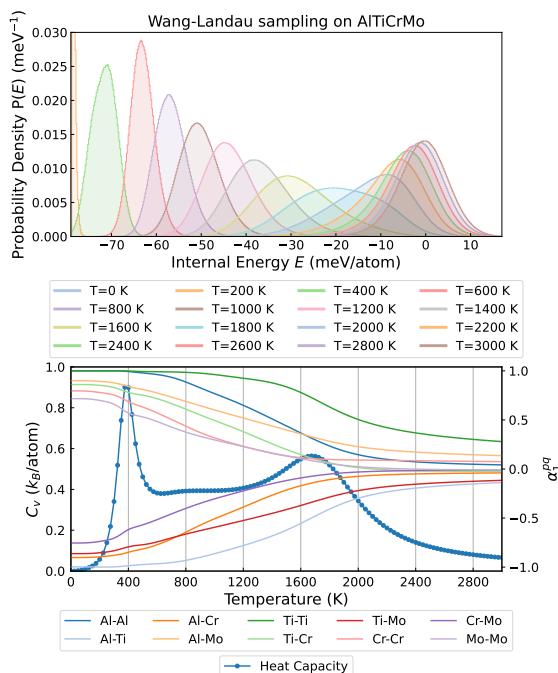


Figure 2: Plots of energy probability distributions, Warren-Cowley ASRO parameters (α_n^{pq}) and simulation heat capacity (C) as a function of temperature for AlTiCrMo obtained using lattice-based Monte Carlo simulations employing Wang-Landau sampling. Here, show α_n^{pq} only for $n = 1$. The zero of the energy scale for the energy histograms is set to be equal to the average internal energy of the alloy obtained at a simulation temperature of 3000 K.

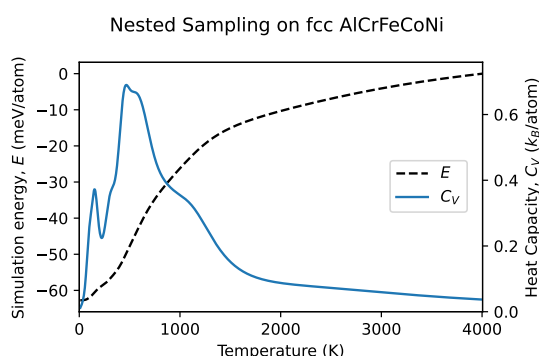


Figure 3: Internal energy, E , and isochoric heat capacity, C_V , obtained using the Nested Sampling algorithm applied to the equiatomic, fcc, AlCrFeCoNi high-entropy alloy. The simulation cell contained 108 atoms. Upon cooling, the initial peak in the heat capacity is associated with an $L1_2$ ordering driven by Al, with subsequent peaks indicating eventual decomposition into multiple competing phases.

Finally, as an example of application of the Nested Sampling algorithm, we consider its application to the AlCrFeCoNi high-entropy alloy, first discussed by Woodgate, Marchant, et

al. (2024). Figure 3 plots the internal energy, E , and isochoric heat capacity, C_V , obtained for the equiatomic, fcc, AlCrFeCoNi system. The simulation cell contained 108 atoms. The initial peak in the heat capacity encountered upon cooling from high temperature is associated with an $L1_2$ ordering driven by Al, with subsequent peaks indicating eventual decomposition into multiple competing phases, which is understood to be consistent with experimental data for this system.

Acknowledgements

H.J.N. and C.D.W. acknowledge invaluable training in scientific software development provided by Dr C. S. Brady and Dr H. Ratcliffe in their Introduction to Scientific Software Development course at the University of Warwick. L.B.P. and C.D.W. acknowledge useful discussions with Dr Georgia A. Marchant (Department of Physics and Astronomy, Uppsala University, Sweden). Finally, C.D.W. acknowledges guidance from Prof. Julie B. Staunton (Department of Physics, University of Warwick, UK) during the early stages of this work.

H.J.N. was supported by a studentship within the Centre for Doctoral Training in Modelling of Heterogeneous Systems, funded by the UK Engineering and Physical Sciences Research Council (EPSRC), Grant EP/S022848/1. L.B.P. acknowledges support from the EPSRC through the individual Early Career Fellowship, Grant EP/T000163/1. C.D.W. acknowledges support from an EPSRC Doctoral Prize Fellowship at the University of Bristol, Grant EP/W524414/1.

Computing facilities for development and testing of the package were provided by the Advanced Computing Research Centre (ACRC) of the University of Bristol, and by the Scientific Computing Research Technology Platform (SCRTP) of the University of Warwick. We also acknowledge use of the Sulis Tier 2 HPC platform. Sulis is funded by EPSRC Grant EP/T022108/1 and the HPC Midlands+ consortium.

References

- Ångqvist, M., Muñoz, W. A., Rahm, J. M., Fransson, E., Durniak, C., Rozyczko, P., Rod, T. H., & Erhart, P. (2019). ICET – A Python Library for Constructing and Sampling Alloy Cluster Expansions. *Advanced Theory and Simulations*, 2(7), 1900015. <https://doi.org/10.1002/adts.201900015>
- Ashton, G., Bernstein, N., Buchner, J., Chen, X., Csányi, G., Fowlie, A., Feroz, F., Griffiths, M., Handley, W., Habeck, M., Higson, E., Hobson, M., Lasenby, A., Parkinson, D., Pártay, L. B., Pitkin, M., Schneider, D., Speagle, J. S., South, L., ... Yallup, D. (2022). Nested sampling for physical scientists. *Nature Reviews Methods Primers*, 2(1), 39. <https://doi.org/10.1038/s43586-022-00121-x>
- Bragg, W. L., & Williams, E. J. (1934). The effect of thermal agitation on atomic arrangement in alloys. *Proceedings of the Royal Society of London. Series A, Containing Papers of a Mathematical and Physical Character*, 145(855), 699–730. <https://doi.org/10.1098/rspa.1934.0132>
- Bragg, W. L., & Williams, E. J. (1935). The effect of thermal agitation on atomic arrangement in alloys-II. *Proceedings of the Royal Society of London. Series A - Mathematical and Physical Sciences*, 151(874), 540–566. <https://doi.org/10.1098/rspa.1935.0165>
- Cowley, J. M. (1950). An Approximate Theory of Order in Alloys. *Physical Review*, 77(5), 669–675. <https://doi.org/10.1103/PhysRev.77.669>
- Cowley, J. M. (1965). Short-Range Order and Long-Range Order Parameters. *Physical Review*, 138(5A), A1384–A1389. <https://doi.org/10.1103/PhysRev.138.A1384>
- Ducastelle, F., & Gautier, F. (1976). Generalized perturbation theory in disordered transitional

- alloys: Applications to the calculation of ordering energies. *Journal of Physics F: Metal Physics*, 6(11), 2039–2062. <https://doi.org/10.1088/0305-4608/6/11/005>
- Khan, S. N., Staunton, J. B., & Stocks, G. M. (2016). Statistical physics of multicomponent alloys using KKR-CPA. *Physical Review B*, 93(5), 054206. <https://doi.org/10.1103/PhysRevB.93.054206>
- Liu, X., Zhang, J., Yin, J., Bi, S., Eisenbach, M., & Wang, Y. (2021). Monte Carlo simulation of order-disorder transition in refractory high entropy alloys: A data-driven approach. *Computational Materials Science*, 187, 110135. <https://doi.org/10.1016/j.commatsci.2020.110135>
- Marchant, G. A., Woodgate, C. D., Patrick, C. E., & Staunton, J. B. (2021). *Ab initio* calculations of the phase behavior and subsequent magnetostriction of $\text{Fe}_{1-x}\text{Ga}_x$ within the disordered local moment picture. *Physical Review B*, 103(9), 094414. <https://doi.org/10.1103/PhysRevB.103.094414>
- Metropolis, N., Rosenbluth, A. W., Rosenbluth, M. N., Teller, A. H., & Teller, E. (1953). Equation of State Calculations by Fast Computing Machines. *The Journal of Chemical Physics*, 21(6), 1087–1092. <https://doi.org/10.1063/1.1699114>
- Naguszewski, H. J., Pártay, L. B., Quigley, D., & Woodgate, C. D. (2025). BraWI: Simulating the thermodynamics and phase stability of multicomponent alloys using conventional and enhanced sampling techniques. *arXiv:2505.05393*. <https://doi.org/10.48550/arXiv.2505.05393>
- Pártay, L. B., Bartók, A. P., & Csányi, G. (2010). Efficient Sampling of Atomic Configurational Spaces. *The Journal of Physical Chemistry B*, 114(32), 10502–10512. <https://doi.org/10.1021/jp1012973>
- Pártay, L. B., Csányi, G., & Bernstein, N. (2021). Nested sampling for materials. *The European Physical Journal B*, 94(8), 159. <https://doi.org/10.1140/epjb/s10051-021-00172-1>
- Rigamonti, S., Troppenz, M., Kuban, M., Hübner, A., & Draxl, C. (2024). CELL: A Python package for cluster expansion with a focus on complex alloys. *Npj Computational Materials*, 10(1), 195. <https://doi.org/10.1038/s41524-024-01363-x>
- Ruban, A. V., Shallcross, S., Simak, S. I., & Skriver, H. L. (2004). Atomic and magnetic configurational energetics by the generalized perturbation method. *Physical Review B*, 70(12), 125115. <https://doi.org/10.1103/PhysRevB.70.125115>
- Shenoy, L., Woodgate, C. D., Staunton, J. B., Bartók, A. P., Becquart, C. S., Domain, C., & Kermode, J. R. (2024). Collinear-spin machine learned interatomic potential for $\text{Fe}_7\text{Cr}_2\text{Ni}$ alloy. *Physical Review Materials*, 8(3), 033804. <https://doi.org/10.1103/PhysRevMaterials.8.033804>
- Singh, P., Smirnov, A. V., & Johnson, D. D. (2015). Atomic short-range order and incipient long-range order in high-entropy alloys. *Physical Review B*, 91(22), 224204. <https://doi.org/10.1103/PhysRevB.91.224204>
- Skilling, J. (2004). Nested Sampling. *AIP Conference Proceedings*, 735, 395–405. <https://doi.org/10.1063/1.1835238>
- Skilling, J. (2006). Nested sampling for general Bayesian computation. *Bayesian Analysis*, 1(4). <https://doi.org/10.1214/06-BA127>
- Van De Walle, A., Asta, M., & Ceder, G. (2002). The alloy theoretic automated toolkit: A user guide. *Calphad*, 26(4), 539–553. [https://doi.org/10.1016/S0364-5916\(02\)80006-2](https://doi.org/10.1016/S0364-5916(02)80006-2)
- Wang, F., & Landau, D. P. (2001). Efficient, Multiple-Range Random Walk Algorithm to Calculate the Density of States. *Physical Review Letters*, 86(10), 2050–2053. <https://doi.org/10.1103/PhysRevLett.86.2050>

- 256 Woodgate, C. D., Hedlund, D., Lewis, L. H., & Staunton, J. B. (2023). Interplay between
257 magnetism and short-range order in medium- and high-entropy alloys: CrCoNi, CrFeCoNi,
258 and CrMnFeCoNi. *Physical Review Materials*, 7(5), 053801. [https://doi.org/10.1103/](https://doi.org/10.1103/PhysRevMaterials.7.053801)
259 [PhysRevMaterials.7.053801](https://doi.org/10.1103/PhysRevMaterials.7.053801)
- 260 Woodgate, C. D., Lewis, L. H., & Staunton, J. B. (2024). Integrated *ab initio* modelling
261 of atomic ordering and magnetic anisotropy for design of FeNi-based magnets. *Npj*
262 *Computational Materials*, 10(1), 272. <https://doi.org/10.1038/s41524-024-01435-y>
- 263 Woodgate, C. D., Marchant, G. A., Pártay, L. B., & Staunton, J. B. (2024). Structure,
264 short-range order, and phase stability of the Al_xCrFeCoNi high-entropy alloy: Insights
265 from a perturbative, DFT-based analysis. *Npj Computational Materials*, 10(1), 271.
266 <https://doi.org/10.1038/s41524-024-01445-w>
- 267 Woodgate, C. D., Naguszewski, H. J., Redka, D., Minár, J., Quigley, D., & Staunton, J.
268 B. (2025). Emergent B2 chemical orderings in the AlTiVNb and AlTiCrMo refractory
269 high-entropy superalloys studied via first-principles theory and atomistic modelling. *Journal*
270 *of Physics: Materials*, 8, 045002. <https://doi.org/10.1088/2515-7639/adf468>
- 271 Woodgate, C. D., & Staunton, J. B. (2022). Compositional phase stability in medium-entropy
272 and high-entropy Cantor-Wu alloys from an *ab initio* all-electron Landau-type theory
273 and atomistic modeling. *Physical Review B*, 105(11), 115124. [https://doi.org/10.1103/](https://doi.org/10.1103/PhysRevB.105.115124)
274 [PhysRevB.105.115124](https://doi.org/10.1103/PhysRevB.105.115124)
- 275 Woodgate, C. D., & Staunton, J. B. (2023). Short-range order and compositional phase
276 stability in refractory high-entropy alloys via first-principles theory and atomistic modeling:
277 NbMoTa, NbMoTaW, and VNbMoTaW. *Physical Review Materials*, 7(1), 013801. <https://doi.org/10.1103/PhysRevMaterials.7.013801>
278 <https://doi.org/10.1103/PhysRevMaterials.7.013801>
- 279 Woodgate, C. D., & Staunton, J. B. (2024). Competition between phase ordering and
280 phase segregation in the Ti_xNbMoTaW and Ti_xVNbMoTaW refractory high-entropy alloys.
281 *Journal of Applied Physics*, 135(13), 135106. <https://doi.org/10.1063/5.0200862>
- 282 Zhang, J., Liu, X., Bi, S., Yin, J., Zhang, G., & Eisenbach, M. (2020). Robust data-driven
283 approach for predicting the configurational energy of high entropy alloys. *Materials &*
284 *Design*, 185, 108247. <https://doi.org/10.1016/j.matdes.2019.108247>